# *In Situ* Detection and Identification of Hesperidin Crystals in Satsuma Mandarin (*Citrus unshiu*) Peel Cells

Tsuyoshi Inoue[a1], Arata Yoshinaga[b], Keiji Takabe[b], Terutaka Yoshioka[c], Kazunori Ogawa[d], Masahiro Sakamoto[a], Jun-ichi Azuma[e] and Yoichi Honda[a]*

* Correspondence to: Y. Honda, Division of Environmental Science and Technology, Graduate School of Agriculture, Kyoto University, Kitashirakawa Oiwake-cho, Sakyo-ku, Kyoto 606-8502, Japan. E-mail: honda@kais.kyoto-u.ac.jp

[a] Division of Environmental Science and Technology, Graduate School of Agriculture, Kyoto University, Kitashirakawa Oiwake-cho, Sakyo-ku, Kyoto 606-8502, Japan

[b] Division of Forest and Biomaterials Science, Graduate School of Agriculture, Kyoto University, Kitashirakawa Oiwake-cho, Sakyo-ku, Kyoto 606-8502, Japan

[c] Citrus Research Division, National Agriculture and Food Research Organization Institute of Fruit Tree Science (NIFTS), 485-6, Okitsunaka-cho, Shimizu-ku, Shizuoka 424-0292, Japan

[d] Grape and Persimmon Research Division, NIFTS, 301-2 Akitsucho-Mitsu, Higashi-hiroshima 739-2494, Japan

[e] Division of Applied Chemistry, Graduate School of Engineering, Osaka University, Yamadaoka, Suita, 565-0871, Japan

[1] A Research Fellowship was provided to Inoue T. by the Japan Society for the Promotion of Science for Young Scientists.

**Keywords**

Albedo; *Citrus unshiu*; flavedo; flavonoid; fruit peel; hesperidin; *in situ* detection; organic crystals; Raman microscopy; scanning electron microscopy

**ABSTRACT:**

Introduction – Hesperidin, a flavonoid known to have important pharmacological effects, accumulates particularly in the peels of satsuma mandarin (*Citrus unshiu*). Although histochemical studies have suggested that hesperidin forms crystals in some tissues of the Rutaceae and Umbelliferae, there has been no rigorous *in situ* detection or identification of hesperidin crystals in *C. unshiu*.

Objective – To characterize the chemical component of the crystals found in *C. unshiu* peels using Raman microscopy.

Methodology – Sections of *C. unshiu* peels were made. The distribution and morphology of hesperidin crystals in the sections were analyzed microscopically. Raman microscopy was used to detect hesperidin in the sections directly.

Results – The crystals were more abundant in immature peel and were observed particularly in areas surrounding vascular bundles, around the border between the flavedo and albedo layers and just below the epidermal cells. In the morphological analysis by scanning electron microscopy (SEM), needle-shaped crystals aggregated and formed clusters of spherical crystals. Spectra obtained by Raman microscopy of the crystals in the peel sections were consistent with those of the hesperidin standard.

Conclusions – This study showed the detailed distribution of crystals in *C. unshiu* peels and the crystals were detected *in situ* and identified the main component of them to be hesperidin using Raman microscopy for the first time.

## Introduction

Flavonoids are one of the major secondary metabolite classes with over 9000 different molecular forms distributed throughout the plant kingdom (Garg *et al*., 2001; Williams and Grayer, 2004; Agati *et al*., 2012). The medical and pharmacological benefits/bioactivities of flavonoids on animal cells have been well documented. The beneficial effects of dietary flavonoids on cancer, cardiovascular diseases and neurodegenerative disorders have attracted much interests in recent years, and the anti-oxidant and anti-inflammatory activities of flavonoids have also been investigated (Williams and Grayer, 2004; García-Mediavilla *et al*., 2007). Meanwhile, roles which flavonoids play in plants have also been focused and studied. For example, flavonoid pigments may serve as pollinator attractants or as signaling molecules functioning in plant-plant and plant-microorganism interactions. The anti-oxidant and UV-protective properties of flavonoids are also well-known, and a role as energy escape valves against excessive lightning has been suggested recently (Hernández and Breusegem, 2010; Agati *et al*., 2012).

Hesperidin, a type of bioflavonoid, is the predominant flavanone that accumulates in plants of the Rutaceae and Umbelliferae, particularly in several *Citrus* peels. In the peels of satsuma mandarin (*Citrus unshiu*), for example, hesperidin is the most accumulated flavonoid followed by narirutin, a hesperidin derivative (Nogata *et al*., 2006). Much attention has been directed to the pharmacological effects of hesperidin including anti-carcinogenic, anti-inflammatory and analgesic activities (Garg *et al*., 2001). Recently, glucosyl hesperidin, a water-soluble form of bioflavonoid, was synthesized and used as a potential drug carrier (Tozuka *et al*., 2011). Although these

numerous effects of hesperidin on animal cells have been studied, the biological activities of hesperidin in plant cells have not been thoroughly investigated.

In several micromorphological studies, various crystals have been found in angiosperms and these crystals generally consist of calcium oxalate and sometimes other calcium salts like calcium citrate in *Mesembryanthemum*, calcium tartrate in the leaves of *Vitis*, calcium malate in *Fraxinus excelsior* and calcium phosphate in *Ceropegia*, *Stapelia* and *Basella* (Metcalfe and Chalk, 1983). Meanwhile, organic crystals occur infrequently and are present in specific plant families. For example, inulin is present in the Asteraceae, berberin in the Berberidaceae and lapachol in the Verbenaceae (Metcalfe and Chalk, 1983). Reports of crystalline flavonoids in plants are more infrequent. Of the wide variety of flavonoids, hesperidin and diosmin crystals were observed in rock samphire (*Crithmum maritimum*), *Citrus limon* and *Barosma betulina* (Cornara *et al*. 2009) and quercetin crystals were found in *Astrophytum* (Iwashina *et al*. 1988). Investigations of these flavonoid crystals were performed by elemental analysis using energy dispersive X-ray spectroscopy, component analysis of the extracts using high performance liquid chromatography (HPLC) (Cornara *et al*., 2009) and UV spectral analysis (Iwashina *et al*., 1988), nevertheless the *in situ* detection and identification of flavonoid crystals have not been accomplished yet.

Raman microscopy has been successfully used to analyze *in situ* various biomolecules in plant tissues (Gierlinger *et al.* 2007 and references therein). For example, coniferin related to cell wall lignification was identified in *Chamaecyparis obtusa* by this technique (Morikawa *et al*., 2010). Raman microscopy was also used to detect flavonoids such as aspalathin from *Aspalathus linearis* (Baranska *et al*., 2006) and carotenoids and flavonoids from *Viola* × *wittrockiana* (Gamsjaegaer *et al*., 2011).

Furthermore, several reports showed the *in situ* detection of crystals at subcellular level using Raman microscopy. A single carotenoid crystal was identified from carrot (*Daucus carota*) cells (Baranska *et al*., 2011) and intracellular calcium oxalate crystals were detected from geraldton waxflower (*Chamelaucium uncinatum*; Macnish *et al*., 2003), which showed that Raman microscopy is a suitable for identifying chemical component of individual crystals presented in living cells of plants..

In this study, we demonstrated that Raman microscopy fulfilled the demands for the *in situ* detection and identification of hesperidin crystals in the peels of *C. unshiu* fruits for the first time. We also investigated the distribution and the morphology of the crystals by light microscopy and scanning electron microscopy (SEM).

## Experimental

### Materials and reagents

Immature fruits of satsuma mandarin (*C. unshiu* Marc. cv. *Aoshima*) were sampled in September 2012, approximately 110 days after flowering, and mature fruits were sampled in December 2012 at approximately 200 days after flowering from an orchard at the National Agriculture and Food Research Organization Institute of Fruit Tree Science in Shizuoka Prefecture, Japan. All fruits were frozen and stored at -20º C until the analyses were conducted. Standards of hesperidin and narirutin were purchased from Extrasynthese S.A. (Genay, France). Analytical grade reagents and solvents were used.

### Sample preparation

Frozen fruits of *C. unshiu* were sliced with a hand knife, and the peels were separated from edible parts. Sections (section 1 and 2; Fig. 1) of small cubes of peel measuring

approximately 5 mm per side were prepared with thicknesses of approximately 30, 40, 50 and 70 μm using a sliding microtome (Yamato Koki Ltd., Asaka, Japan). The sections were stained with borax methylene blue solution [1.0% (w/v) methylene blue in 1.0% (w/v) borax] for light microscopy or air-dried for SEM observation. For Raman microscopy, the sections were placed on a glass slide with a drop of distilled water, covered with a coverslip, and sealed with nail polish to avoid evaporation of distilled water during measurements.

**Light microscopy**

Sections were stained with borax methylene blue solution for 1 min at room temperature, washed with ethanol three times, passed through xylene and mounted in Canada balsam. Distribution of hesperidin crystals were observed under a light microscope (Olympus BX51, Tokyo, Japan). The cells and crystals from the image of immature peel section were manually traced using Adobe Photoshop and their diameters at the maximum and minimum equators were measured by the ellipse approximation using NIH ImageJ 1.48v program (developed at the United States National Institutes of Health and available on the Internet at http://rsb.info.nih.gov/ij/).

**Fluorescence microscopy**

Some sections were observed using a fluorescence microscope (Olympus BX51, Tokyo, Japan) with an Omega XF06 filter set consisting of a exciter XF1005 (365WB50), dichroic XF2001 (400DCLP) and emitter XF3002 (450DF65; Omega Optical Inc., Brattleboro, VT, USA).

145 **Scanning electron microscopy (SEM)**

146 Immature fruit peel sections were sputter-coated with gold using an ion coater
147 (JEE-1100E, JEOL Ltd., Akishima, Japan) and observed using a SEM (JSM-6060,
148 JEOL Ltd., Akishima, Japan) at an accelerating voltage of 5 kV.

149

150 **Raman microscopy**

151 The equipment and protocols used were reported by Morikawa *et al*. (2010). A Raman
152 microprobe spectrometer (LabRam HR 350V, Horiba Jobin Yvon, Kyoto, Japan)
153 equipped with a confocal microscope (Olympus BX40) and an air-cooled
154 charge-coupled device detector (Andor Technology, Belfast, Northern Ireland) was
155 employed for the analysis. A 633 nm laser was used to excite the sample through a 50X
156 objective (Olympus, MPlan, 50X/N.A. 0.75). The laser power was 6.7 mW at the
157 samples, integration time was 1.0 sec and the number of accumulation was 50. The
158 confocal aperture was 800 μm. Spectral data in the range of 400-3200 $cm^{-1}$ were
159 analyzed by LabSpec 4.18 software with baseline correction. Raman spectrometer was
160 calibrated with the spectrum at 520 $cm^{-1}$ from silicon wafer and the peak position
161 accuracy was estimated by triplicate measurements of hesperidin and narirutin standards.
162 Raman spectra were taken from crystalline materials in 50 μm thick sections (section 2)
163 after repeated laser irradiation to decrease background fluorescence from the section
164 that disturbed the detection of the unique hesperidin spectrum. The crystalline materials
165 were also collected from sections soaked in 50 μL of distilled water and ultrasonicated.
166 Spectra of the collected crystals were taken for comparison. For positive controls,
167 standards of hesperidin and narirutin were also analyzed. All scans were repeated to
168 obtain suitable signal-to-noise ratios.

## Results and discussion

### Distribution of crystals in *C. unshiu* peels observed by light microscopy

Light micrographs of the 40 and 50 μm thick sections (section 1 and 2) of *C. unshiu* peels are shown in Fig. 2. *Citrus* peels consist of a colored outer layer containing oil glands called the flavedo and an inner white spongy layer called the albedo. The albedo layer accounted for larger areas than the flavedo layer in the immature peel but were more fragile in the mature peel. In the flavedo tissue, the oil glands enlarged as the peels matured. Innumerable green-stained structures were observed in the immature peel; however, fewer and smaller green-stained structures were present in the mature peel (Fig. 2). The structures showed crystalline properties that were confirmed using polarizing light microscopy (data not shown). In particular, the crystals accumulated in areas surrounding vascular bundles, around the border between the flavedo and the albedo layers (Fig. 2a, b, 3a), and just below the epidermal cells (Fig. S1).

Occurrence of the crystals correlated with immature peel sections thicker than 40 μm, however the number of observed crystals significantly decreased in 30 μm sections (data not shown). The measured diameters at the maximum and minimum equators of cells from the 40 μm thick section (section 2) of the immature peel were 44.2 ± 4.7 and 34.2 ± 3.9 μm (n = 20), respectively. And those values of the crystals were 45.3 ± 20.1 and 35.8 ± 14.4 μm (n = 45), respectively. These results suggested the appropriate thickness of the peel section was approximately over 40 μm for observing the proper distribution of the crystals. In the mature peels, there was no clear relationship between the number of crystals and the thickness of the sections.

The distribution of the crystals was not homogenous in immature peel sections

193 (Fig. 2a, b), making it difficult to quantify the density. In mature peel sections, albedo
194 tissues were too fragile to section using the sliding microtome (Fig. 2d, e). Although a
195 paraffin-embedding protocol may be an alternative sectioning method, the loss of
196 crystals in thin sections under 30 μm might preclude obtaining accurate distribution data
197 using this protocol.

198 The solubility properties of the crystals in the sections were investigated. The
199 crystals were found to be insoluble in distilled water but soluble in dimethyl sulfoxide
200 (DMSO) (Fig. 3a, b). Hesperidin showed a poor water solubility (4.95 ± 0.99 μg/mL;
201 Majumdar and Srirangam, 2009) and DMSO and DMSO/methanol (1:1, v/v) were often
202 used as solvents to extract hesperidin for quantitative analyses (Lee, 2000; Nogata *et al*.
203 2006; Inoue *et al*., 2010). Therefore, the properties of the crystals were similar to those
204 of hesperidin. The comparatively strong fluorescence of sections decreased significantly
205 after soaking the section in distilled water for a few hours, leaving only the weak
206 intrinsic fluorescence of lignin in the vascular bundles (Fig. 3c, d). Because the crystals
207 showed little fluorescence and remained still in the sections after washing with distilled
208 water, this result suggested that there were other fluorescent components besides the
209 crystals in the peels. We are now investigating these water-soluble and fluorescent
210 compounds for the identification as one of our future issues.

211

212 **Fine structure of crystals observed by SEM**

213 SEM observations yielded minute descriptions of the crystals accumulating in the peel
214 (Fig. 4). Needle-shaped crystals aggregated to form clusters of spherical crystals, which
215 were attached to the cell walls (Fig. 4a-c). The needle-shaped crystals were
216 morphologically consistent with the structure of the hesperidin standard crystal (Fig.

4d).

**Comparison of Raman spectra of crystals, hesperidin and narirutin**

Raman spectra were taken from crystals in immature peels of *C. unshiu* and compared to the spectra of hesperidin and narirutin standards (Fig. 5, S2). When hesperidin and narirutin standards were analyzed, the peaks at 764 and 1607 $cm^{-1}$ were found in the spectrum from hesperidin standard and the peak at 812 $cm^{-1}$ was found in that from narirutin standard (Fig. 5c, d). The ranges of the main seven Raman peaks from hesperidin standard and the six peaks from narirutin standard by triplicate measurements were 6.2-0.2 and 3.4-0.1 $cm^{-1}$, respectively. Therefore, hesperidin standard showed two specific Raman peaks and narirutin standard showed one specific peak, which suggested that these two standards are distinguishable by Raman microscopy. Then, the Raman spectrum of a crystal in the peel section was compared to those of the standards and these spectra were found to be similar (Fig. 5a, c). The main peaks from the crystal at 767, 1296, 1604, 1644, 2895, 2935 and 3079 $cm^{-1}$ were equivalent to the peaks from the hesperidin standard at 764, 1293, 1607, 1638, 2897, 2933 and 3074 $cm^{-1}$, respectively (Fig. 5a, c). The gap of their Raman shift between the crystals and hesperidin standard were within the range of the main Raman peaks from hesperidin standards in triplicated measurements (6.2-0.2 $cm^{-1}$). Therefore, these results strongly suggested the main component of the crystals to be hesperidin.

In Raman spectra taken from aromatic compounds, the aromatic C-H our-of-plane deformation vibration is assigned to the spectra in the region 900-650 $cm^{-1}$ and aromatic C-H and ring C=C stretching vibrations are assigned to them in the region 3080-3010 $cm^{-1}$ and 1625-1590 $cm^{-1}$, respectively (George, 2001). According to the knowledge, the

241 Raman peaks shown in Fig. 5 of hesperidin and the crystals in peel cells at 764/767,
242 3074/3079, and 1607/1604 $cm^{-1}$ are due to the C-H our-of-plane vibrations of the
243 aromatic ring and the stretching vibration of C-H and C=C bonds, respectively. The
244 Raman spectra of crystals isolated from sections by ultrasonication were compared to
245 the spectra of the crystals remainded *in situ* (Fig. 5a, b). Both spectra had common
246 peaks corresponding to the spectrum of hesperidin standard and there was no significant
247 influence of the background using Raman microscopy.
248
249 **Localization of hesperidin crystals and the prospect of their dynamics and roles in**
250 **plants**
251 The hesperidin content of immature and mature *C. unshiu* peels was reported to be 64.3
252 ± 0.5 mg/g fresh weight (FW) and 18.8 ± 0.1 mg/g FW, respectively (Inoue *et al*., 2010).
253 Nogata *et al*. (2006) reported that there is a lower concentration of hesperidin in the
254 flavedo layer than in the albedo layer in several kinds of mature *Citrus* fruits. Moriguchi
255 *et al*. (2001) showed that the hesperidin content decreased with the ripening of *C.*
256 *unshiu* fruits; the hesperidin content in the albedo layer was 60 mg/g FW and decreased
257 to 30 mg/g FW during maturation, whereas the hesperidin content of the flavedo layer
258 decreased from 20 to 10 mg/g FW during fruit development. The distribution pattern of
259 crystals identified by our light microscopy analyses was consistent with the results of
260 the quantitative component analyses reported by Moriguchi *et al*. (2001), Nogata *et al*.
261 (2006) and Inoue *et al*. (2010). Although most analytical studies used ground tissue
262 samples for extraction provide several quantitative data, they might lose detailed
263 information about the distribution pattern of components. *In situ* detection of
264 components compensates for the quantitative analyses and provides a more

comprehensive understanding of the dynamics, localization and role of the components in plant.

Numerous crystals of hesperidin sometimes were located around the vascular bundles of immature peels (Fig. 2a, 3a). Cornara *et al*. (2009) also showed that hesperidin and diosmin crystals were mainly located near the phloem and in vessels of the vascular bundles of *C. maritimum* leaves and suggested the intercellular transport of these flavonoids. Long distance movement of flavonoids through the vascular systems of plants is controversial. Castillo *et al*. (1992) showed that neohesperidin and naringin were in the phloematic fluids of *Citrus aurantium*. However, hesperidin is water-insoluble and is assumed to crystallize near the synthesized position. It may be plausible that substrates, such as sugars, are transported through vascular bundles and utilized for the synthesis of hesperidin in the nearby cells, which leads to the aggregated crystals observed near the vascular bundles.

In the flavedo layer of *Citrus clementina*, Matas *et al*. (2010) showed that several flavonoid biosynthesis related genes are expressed predominantly in the epidermal cells and not in sub-epidermal cells of the peels. Comparing to our results, this gene expression pattern may approximetly correspond to the distribution pattern of hesperidin crystals in immature *C. unshiu* peels that comparatively large clusters of crystals were observed just below the epidermal cells but not in the sub-epidermal cell layer (Figure S1). In the albedo layer of *C. unshiu* immature peels, in contrast, larger clusters of hesperidin crystals were accumulated particularly in the outer albedo layer or around the border between the flavedo and albedo layers (Figure 2b). The difference of flavonoid biosynthesis related gene expression pattern within the albedo layer has not been reported and could be an interesting theme.

289 Among several roles proposed for hesperidin in plants, Homma *et al*. (1992) and
290 Alves *et al*. (2009) suggested that the needle-shaped crystals could respond to infections
291 by *Diaporthe citri* and *Xylella fastidiosa* in *C. unshiu* and *C. sinensis*, respectively. The
292 crystals, which were identified as hesperidin by Homma *et al*. (1992) but have not yet
293 been characterised by Alves *et al*. (2009), filled up the xylem vessels of infected fruits
294 and leaves and obstructed the penetration of fungal hyphae or the formation of biofilm
295 by the bacterium, respectively. In these cases, *in situ* detection and identification of
296 hesperidin crystals by our methodology would be an effective means to identify the
297 crystals. We also verified the presence of hesperidin crystals in healthy fruits of *C.*
298 *unshiu*, therefore other functional roles of hesperidin should be considered in future
299 investigations.
300 In this study, we focused on the characteristic property of hesperidin to form
301 clusters of spherical crystals in *C. unshiu* peels, thereby facilitating the *in situ* detection
302 and identification of the crystals as hesperidin for the first time. Furthermore, the
303 detailed distribution pattern of hesperidin crystals observed in this investigation
304 provided some clues of comprehensive understanding about the dynamics and/or the
305 roles of hesperidin in *Citrus* that may also offer insights into the unknown functional
306 roles of flavonoids in plants.
307
308 **References**
309 Agati G, Azzarello E, Pollastri S, Tattini M. 2012. Flavonoids as antioxidants in plants:
310 Location and functional significance. *Plant Sci* **196**: 67-76.
311 Alves E, Leite B, Pascholati SF, Ishida ML, Andersen PC. 2009. *Citrus sinensis* leaf
312 petiole and blade colonization by *Xylella fastidiosa*: Details of xylem vessel

313 occlusion. *Sci Agri (Piracicaba, Braz)* **66**(2): 218-224.
314 Baranska M, Schulz H, Joubert E, Manley M. 2006. *In situ* flavonoid analysis by
315 FT-raman spectroscopy: identification, distribution, and quantification of aspalathin
316 in green rooibos (*Aspalathus linearis*). *Anal Chem* **78**: 7716-7721.
317 Baranska M, Baranski R, Grzebelus E, Roman M. 2011. In situ detection of a single
318 carotenoid crystal in a plant cell using Raman microspectroscopy. *Vib Spectrosc* **56**:
319 166-169.
320 Castillo J, Benavente O, Del Rio JA. 1992. Naringin and neohesperidin levels during
321 development of leaves, flower buds, and fruits of *Citrus aurantium*. *Plant Physiol*
322 **99**(1): 67-73.
323 Cornara L, D'arrigo C, Pioli F, Borghesi B, Bottino C, Patrone E, Mariotti MG. 2009.
324 Micromorphological investigation on the leaves of the rock samphire (*Crithmum*
325 *maritimum* L.): Occurrence of hesperidin and diosmin crystals. *Plant Biosyst*
326 **143**(2): 283-292.
327 Gamsjaeger S, Baranska M, Schulz H, Heiselmayere P, Musso M. 2011. Discrimination
328 of carotenoid and flavonoid content in petals of pansy cultivars (*Viola* x
329 *wittrockiana*) by FT-Raman spectroscopy. *J Raman Spectrosc* **42**: 1240–1247.
330 García-Mediavilla V, Crespo I, Collado PS, Esteller A, Sánchez-Campos S, Tuñón MJ,
331 González-Gallego J. 2007. The anti-inflammatory flavones quercetin and
332 kaempferol cause inhibition of inducible nitric oxide synthase, cyclooxygenase-2
333 and reactive C-protein, and down-regulation of the nuclear factor kappaB pathway
334 in Chang Liver cells. *Eur J Pharmacol* **557**: 221-229.
335 Garg A, Garg S, Zaneveld LJD, Singla AK. 2001. Chemistry and pharmacology of the
336 citrus bioflavonoid hesperidin. *Phytother Res* **15**: 655-669.

George S. 2001. *Infrared and Raman Characteristic Group Frequencies: Tables and Charts* (2nd Edn.). Wiley: New York; 157-167.

Gierlinger N, Schwanninger M. 2007. The potential of Raman microscopy and Raman imaging in plant research. *Spectroscopy* **21**: 69–89.

Hernández I, Breusegem FV. 2010. Opinion on the possible role of flavonoids as energy escape valves: Novel tools for nature's Swiss army knife? *Plant Sci* **179**: 297-301.

Homma Y, Ohsawa T, Arimoto Y, Takahashi H. 1992. Chemical structure of preinhibitin in citrus stem-end rot. *Plant Pathol* **82**: 310-314.

Inoue T, Tsubaki S, Ogawa K, Onishi K, Azuma J. 2010. Isolation of hesperidin from peels of thinned *Citrus unshiu* fruits by microwave-assisted extraction. *Food Chem* **123**: 542-547.

Iwashina T, Ootani S, Hayashi K. 1988. On the pigmented spherical bodies and crystals in tepals of cactaceous species in reference to the nature of betalains or flavonols. *Bot Mag Tokyo* **101**: 175-184.

Lee SH. 2000. HPLC analysis of phenolic compounds. In *Food Analysis by HPLC* (2nd Edn.). Nollet MLL (Ed.). Marcel Dekker: New York; 775-824.

Macnish AJ, Irving DE, Joyce DC, Vithanage V, Wearing AH, Webb RI, Frost RL. 2003. Identification of intracellular calcium oxalate crystals in *Chamelaucium unicinatum* (Myrtaceae). *Aust J Bot* **51**: 565-572.

Majumdar S, Srirangam R. 2009. Solubility, stability, physicochemical characteristics and *in vitro* ocular tissue permeability of hesperidin: a natural bioflabonoid. *Pharm Res* **26**(5): 1217-1225.

Matas A, Agusti J, Tadeo FR, Talón M, Rose JKC. 2010. Tissue-specific transcriptome profiling of the citrus fruit epidermis and subepidermis using laser capture

361 microdissection. *J Exp Bot* **61**(12): 3321-3330.
362 Metcalfe CR, Chalk L. 1983. *Anatomy of the Dicotyledons: Wood Structure and*
363 *Conclusion of the General Introduction* (Vol. 2, 2nd Edn.). Clarendon Press: Oxford;
364 82-97.
365 Moriguchi T, Kita M, Tomono Y, Endo-Inagaki T, Omura M. 2001. Gene expression in
366 flavonoid biosynthesis : Correlation with flavonoid accumulation in developing
367 citrus fruit. *Physiol Plantarum* **111**: 66-74.
368 Morikawa Y, Yoshinaga A, Kamitakahara H, Wada M and Takabe K. 2010. Cellular
369 distribution of coniferin in differentiating xylem of *Chamaecyparis obtusa* as
370 revealed by Raman microscopy. *Holzforschung* **64**: 61-67.
371 Nogata Y, Salamoto K, Shiratsushi H, Ishii T, Yano M, Ohta H. 2006. Flavonoid
372 composition of fruit tissues of citrus species. *Biosci Biotechnol Biochem* **70**(1):
373 178-192.
374 Tozuka Y, Imono M, Uchiyama H, Takeuchi H. 2011. A novel application of
375 α-glucosyl hesperidin for nanoparticle formation of active pharmaceutical
376 ingredients by dry grinding. *Eur J Pharm Biopharm* **79**: 559-565.
377 Williams CA, Grayer RJ. 2004. Anthocyanins and other flavonoids. *Nat Prod Rep* **21**:
378 539-573.

**FIGURE**

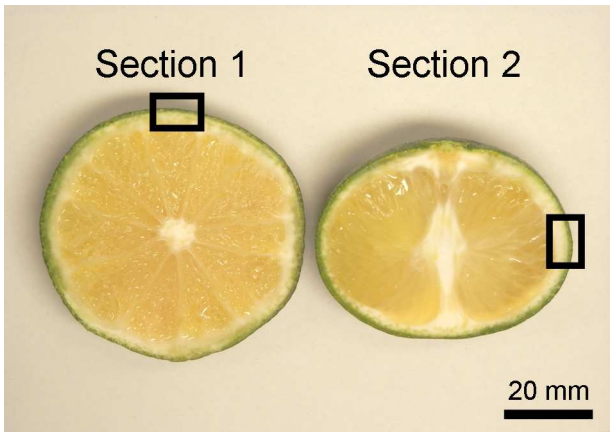


**Figure 1.** *C. unshiu* immature fruit. A section (left; section 1) and a section (right; section 2) of *C. unshiu* fruit. The regions in rectangular boxes identify examples of sampling locations for sections.

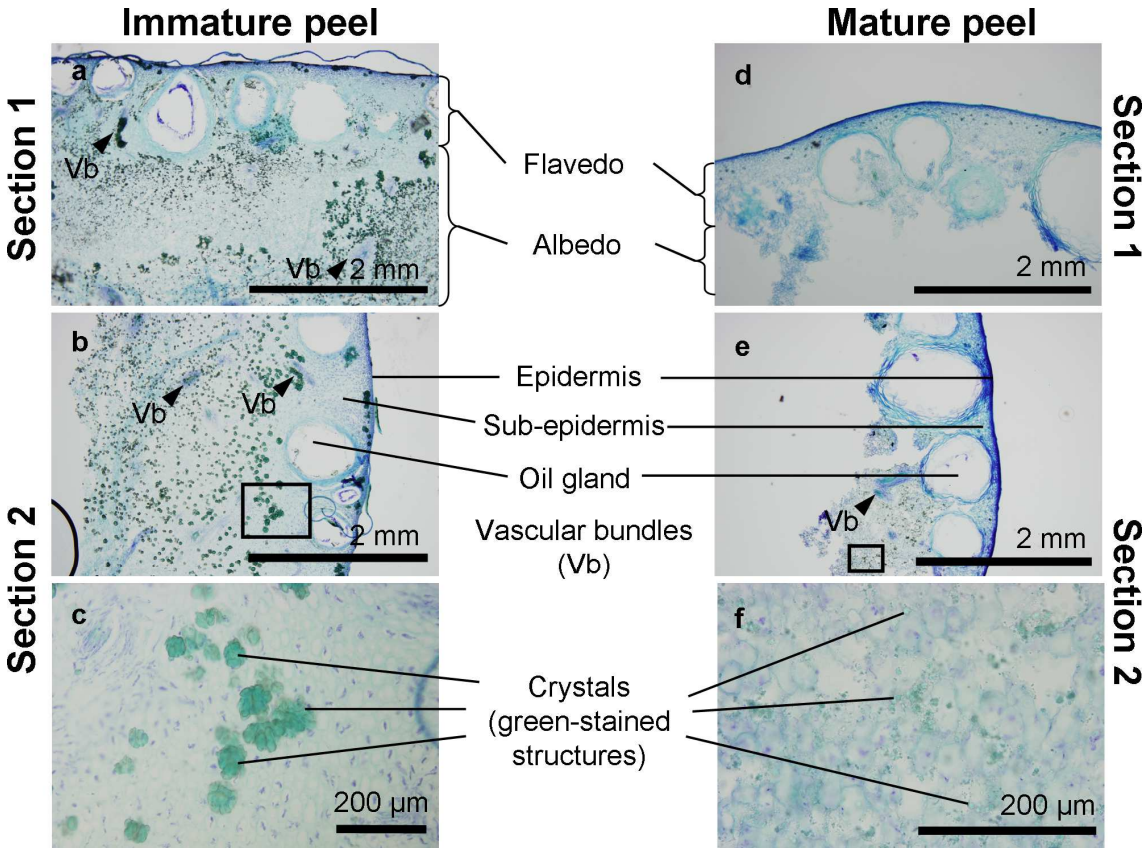


**Figure 2.** Light micrographs of the sections taken from *C. unshiu* peels. Sections (section 1: a, d; section 2: b, c, e, f) of the immature (a-c) and mature (d-f) peels were stained with a borax methylene blue solution. Numerous green-stained structures in the sections represent the crystals and the squares in (b) and (e) represent magnified images shown in (c) and (f), respectively. Arrowheads show the presence of vascular bundles (Vb). (a-c) section thickness = 40 µm and (d-f) section thickness = 50 µm.

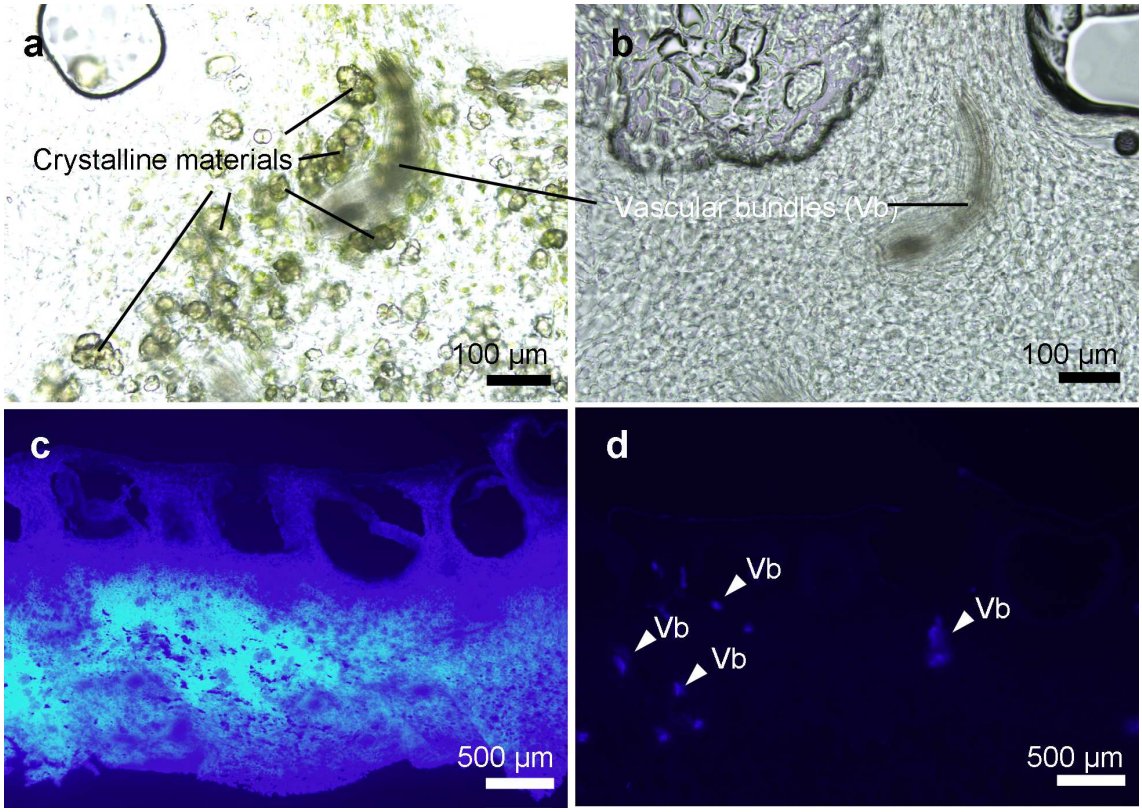


**Figure 3.** Light and fluorescence micrographs of sections (section 1) of *C. unshiu* immature peels. Numerous crystals were observed around the vascular bundles (Vb) in a section soaked in distilled water (a), but after washing with DMSO, the crystals were not observed in the section (b). An air-dried section (c) had strong fluorescence in broad areas in the albedo, but after washing with distilled water, only the fluorescence of the vascular bundles containing lignin remained (d). (a-d) section thickness = 50 µm.

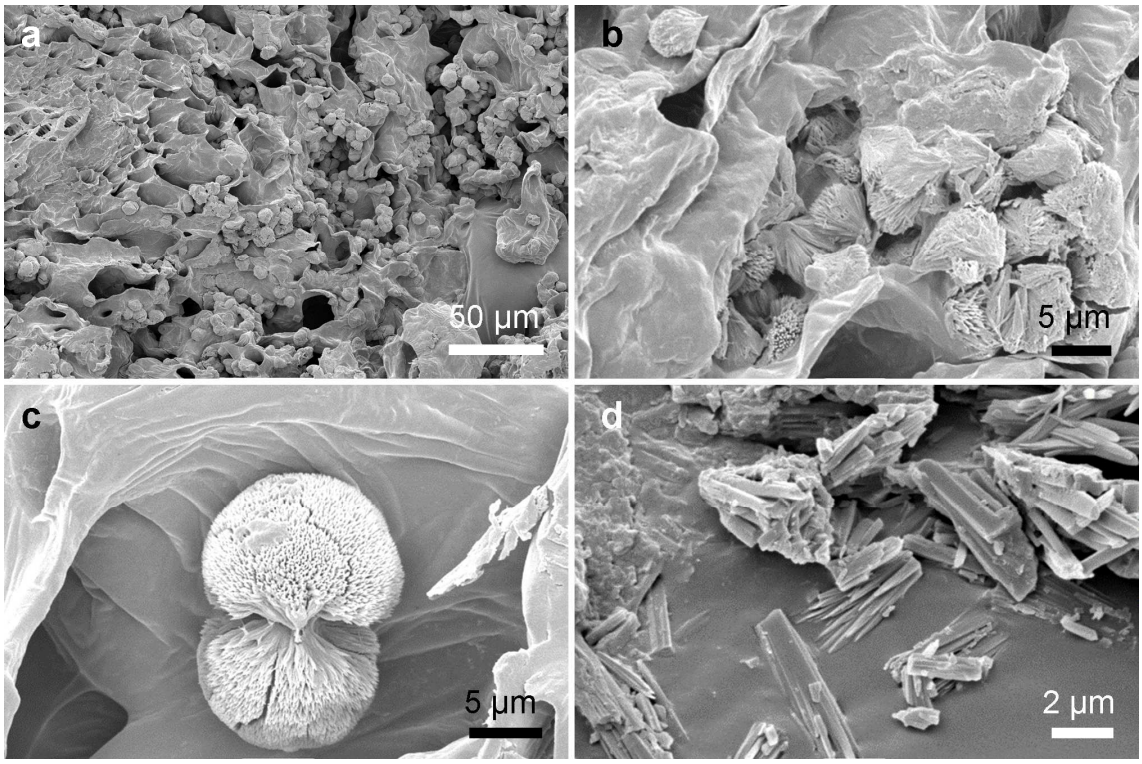


**Figure 4.** SEM micrographs of sections of *C. unshiu* immature peel and a hesperidin standard. In the immature peel of 50 µm thick sections (a-d), numerous needle-shaped crystals (b) aggregated to form spherical crystals (a, c) and many clusters were attached to the surface of the peel section (a). Needle-shaped crystals from a hesperidin standard (d).

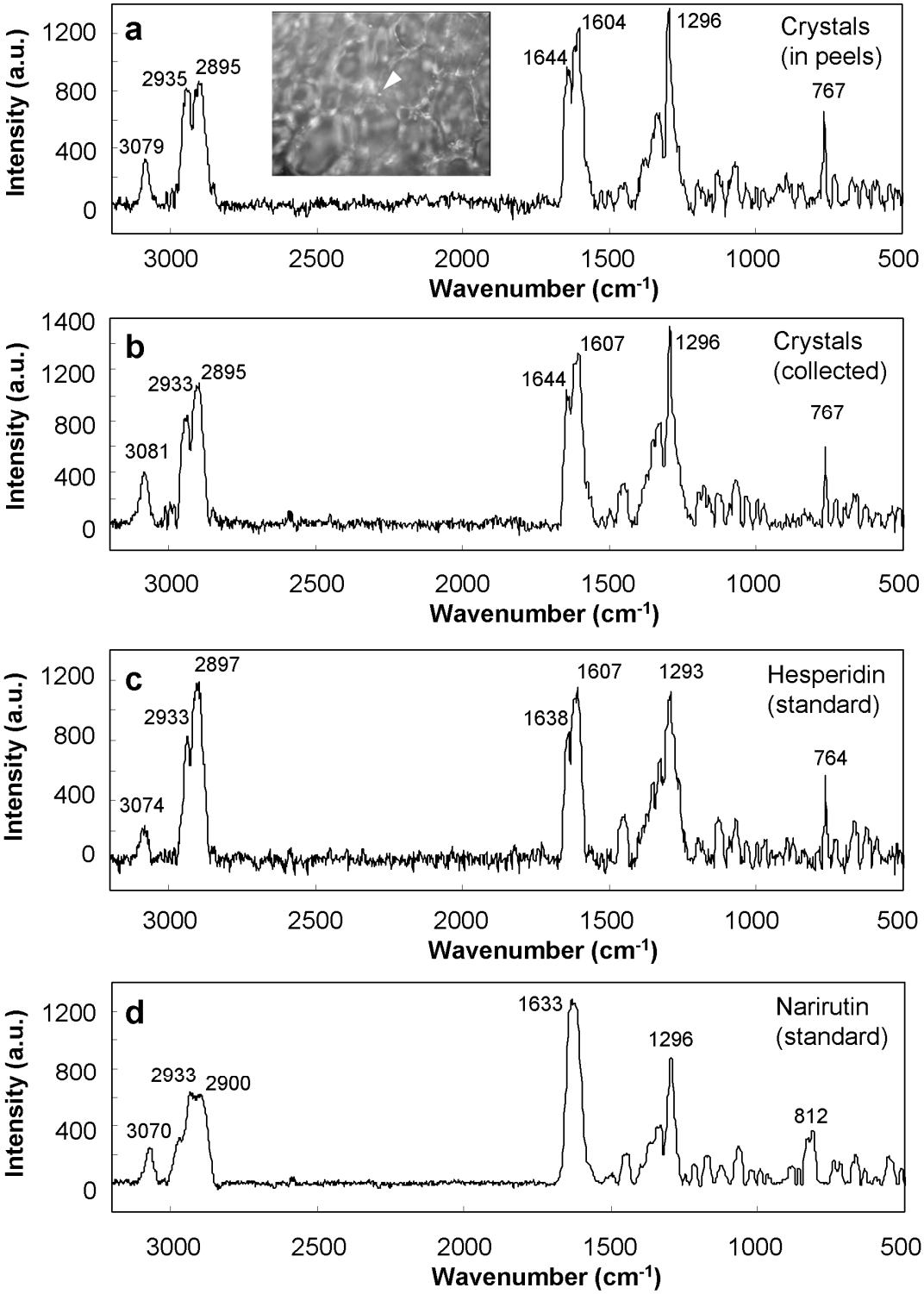


**Figure 5.** Raman spectra from a crystal in a section of *C. unshiu* immature peel, another crystal collected using ultrasonication, hesperidin and narirutin standards. Wavenumbers

of the major peaks are indicated for each spectrum, crystals in peels (a), collected crystals (b), hesperidin standard (c) and narirutin standard (d). The white arrow in the inset of (a) shows the position where the crystal spectrum was taken. The spectral data shown are baseline corrected.

## Supplementary material

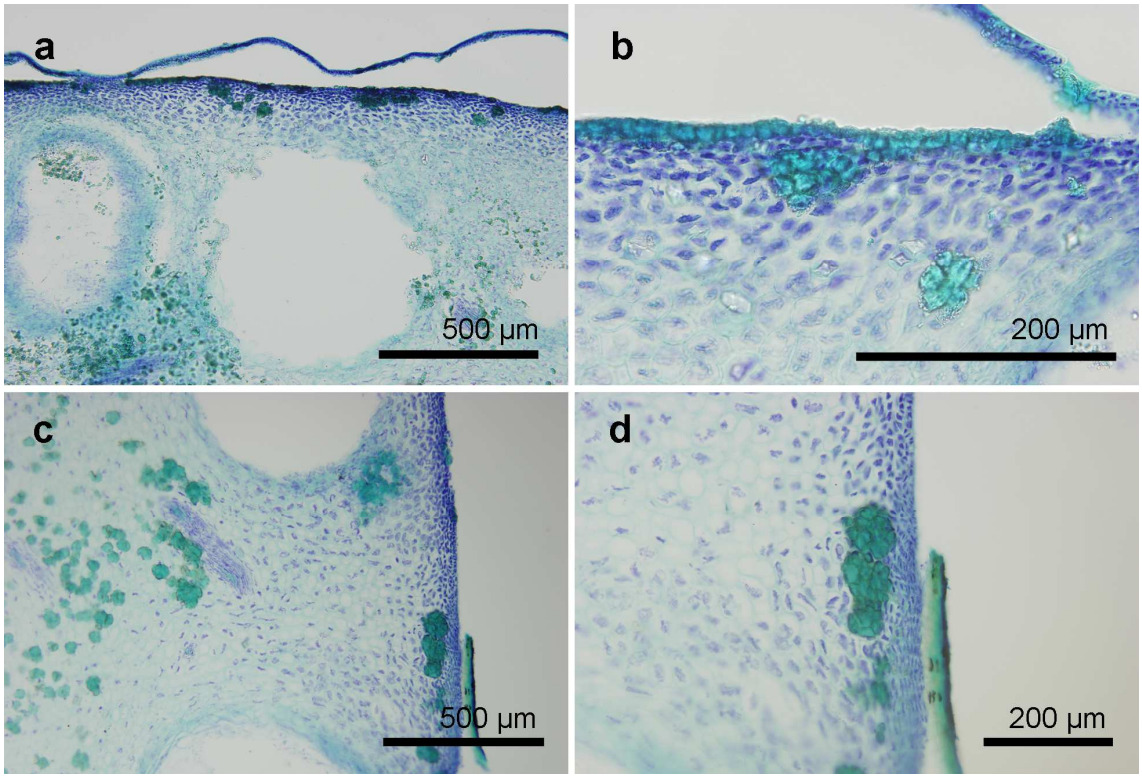


**Figure S1.** Light micrographs of the sections taken from *C. unshiu* peels. Sections (section 1: a, b; section 2: c, d) of the immature peels were stained with a borax methylene blue solution. Large cluster of the crystals were found just below the epidermal cells. (a-d) section thickness = 40 µm.

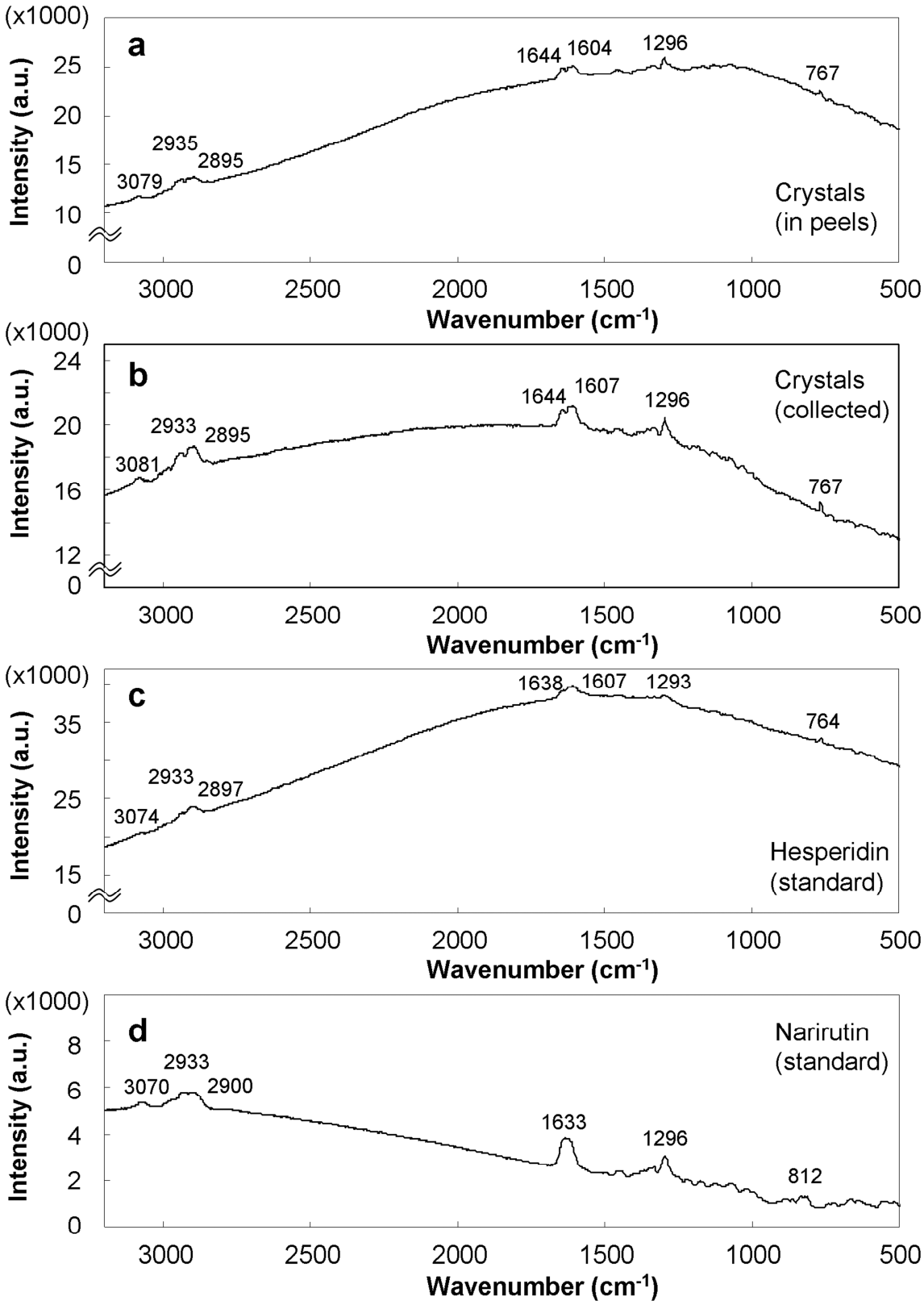


**Figure S2.** Original Raman spectra from a crystal in a section of *C. unshiu* immature

peel, another crystal collected using ultrasonication, hesperidin and narirutin standards. Wavenumbers of the major peaks are indicated for each spectrum, crystals in peels (a), collected crystals (b), hesperidin standard (c) and narirutin standard (d).